Shoulder bone geometry affects the Glenohumeral joint active and passive axial rotational range

Abstract

Background:

The range-of-motion of the Glenohumeral joint varies substantially between individuals and is dependent on humeral position. How variation in shape of the humerus and scapula affects shoulder axial range-of-motion at various positions has not been previously established.

Hypothesis/Purpose:

The aim of this study is to quantify variation in the shape of the Glenohumeral joint and investigate whether the scapula and humerus geometries affect axial rotational range of the Glenohumeral joint.

Study Design: Cross-sectional study

Methods:

The range of active and passive internal-external rotation of the Glenohumeral joint was quantified for 10 asymptomatic subjects using optical motion tracking at 60º, 90º and 120º humeral elevations in the Coronal, Scapular and Sagittal planes. Bone geometrical parameters were acquired from shoulder MRI scans and correlations between geometric parameters and maximum internal and external rotations were investigated. Three-dimensional subject-specific models of the humerus and scapula were used to identify collisions between bones at the end-of-range.

Results:

Maximum internal and external rotations of the Glenohumeral joint were correlated to geometrical parameters and were limited by bony collisions. Generally, the active axial rotational range was greater with increased articular cartilage and glenoid curvature; whilst a

shorter acromion resulted in greater passive range. Greater internal rotation was correlated with a greater glenoid depth and curvature in the Scapular plane (r=0.76, p<0.01 at 60° elevation), a greater subacromial depth in the Coronal plane (r=0.74, p<0.01 at 90° elevation), and a greater articular cartilage curvature in the Sagittal plane (r=0.75, p<0.01 at 90° elevation). At higher humeral elevations, a greater subacromial depth and shorter acromion allowed a greater range-of-motion.

Conclusion:

The study strongly suggests that specific bony constraints restrict the maximum internal and external rotations achieved in active and passive glenohumeral movement.

Clinical Relevance:

This study identifies bony constraints which limit the range-of-motion of Glenohumeral joint. This information can be used to predict full range-of-motion and set patient specific rehabilitation targets for patients recovering from shoulder pathologies. It can improve positioning and choice of shoulder implants during pre-operative planning by considering points of collision which could limit range-of-motion.

Key Terms: Glenohumeral joint, Kinematics, Bone geometry, Axial rotation, Range-of-motion.

What is known about the subject?

The maximum internal and external rotation of the Glenohumeral joint is dependent on the elevation angle and elevation plane of the humerus and there is large variation in the range-of-motion between individuals[15]. Previous research has shown osseous adaptation at the proximal humerus can lead to an increased angle of retroversion in elite overhead sports athletes, which has been related to an increased range of external rotation of the Glenohumeral joint. However, the relationship between the Glenohumeral joint bone geometry and the available ranges of active and passive internal and external rotation has not been previously defined.

What this study adds to existing knowledge:

This study brings new insight on how normal variation in the shape of the humerus and scapula bones affect the Glenohumeral joint range-of-motion at multiple humeral planes and elevation angles; thus mapping this effect over the normal range of shoulder movement. This will contribute to better understanding of the shoulder joint movement and function and has implications on performance analysis of overhead sports athletes, development and design of implants and developing personalised rehabilitation targets for patients with shoulder disorders.

Introduction

The maximum internal and external rotation of the Glenohumeral joint (GHJ) varies between individuals[15] and is dependent on the elevation angle and elevation plane of the humerus[15]. The range of axial rotation is reduced at higher humero-thoracic elevations and in the Sagittal plane compared to the Coronal and Scapular planes and is shown to be greater during passive rotations compared to active movement[15]. Previous studies have demonstrated that the range-of-motion of the GHJ is affected by ligamentous and muscular constraints[11,17,27], and can also be compromised by injury and pathology[9]. There is also some limited evidence that the range of motion of the joint is limited by the collision[20] and shape of bones that form the articulation[14]. However, the nature of the relationship between bone shape of the humerus and scapula and the axial range-of-motion of the GHJ remains unclear. Before investigating the effect of soft tissue restraints on the range-of-motion of the GHJ and shoulder pathologies, it is vital to have an understanding of the full range that can be achieved given the limitations imposed by bone shape. Describing the relationship between bone shape and range-of-motion can be used to define patient-specific rehabilitation targets following soft-tissue injury and also in the development and design of shoulder prostheses as well as in optimising implant positioning to achieve a greater, more natural range of motion.

Previous *in-vitro* studies have shown that the maximum internal and external rotation that can be achieved at the joint is influenced by muscular constraints and joint conformity during active motion[17], and that passive range-of-motion is influenced by ligamentous[22] and bony[14] constraints. The study conducted by Chopp-Hurley *et al.* used advanced probabilistic approaches to model variation in the subacromial depth, suggesting that at higher humeral elevations the subacromial depth is reduced, which may affect the range-of-motion of the GHJ as a result of soft-tissue impingement[5]. Differences in the axial range-of-motion are thought to be influenced by the conformity of the GHJ during active axial rotation, when the joint is compressed, and by the shape of the humeral tuberosity and acromion during passive axial rotation following translation of the humeral head[15].

Understanding the bony constraints of the GHJ can improve the design and positioning of shoulder implants. Scans of the shoulder have been used to create subject-specific computer bone models of the GHJ from segmented bone images to predict patient specific ranges-of-motion[19]. Krekel *et al*. used collision detection simulations from segmented CT scans to visualise the range-of-motion of the GHJ in response to changes in positioning of the patient's shoulder prosthesis, allowing surgical outcomes to be optimised through pre-operative planning of shoulder athroplasty[19]. Although previous studies have acquired geometrical parameters to describe the shape of the humerus and scapula at the GHJ[10,12,13,30], these have not yet related bone geometry to *in-vivo* kinematics and have not described the bony constraints which limit the range of axial rotation of the GHJ.

The study will investigate the relationship between the GHJ bone geometry and the GHJ active and passive ranges of internal and external rotation in an asymptomatic group to further understand the role of bony restraints of the GHJ. This will be carried out by measuring two-dimensional and three-dimensional bone geometrical parameters of the humerus and scapula, including the articular cartilage, from MRI scans of the shoulder and testing for correlations between these geometrical parameters and ranges-of-motion. A 3D subject-specific model will also be used to observe the points of bony collision which limit the maximum internal and external rotations at various humeral positions.

Materials and Methods

Data collection

Kinematic data and MRI scans were acquired from 10 healthy subjects (5 male, 5 female; age, 27 ± 5 years; weight, 76 ± 21 kg). Subjects had no history of shoulder pathology or surgery, had no instability of the shoulder and had no recent shoulder pain. Subjects had no difficulty completing activities of daily living and did not regularly participate in overhead sports activities. They also met the inclusion criteria for MRI scanning as defined according to standard clinical practice. The study was approved by the National Research Ethics Service and the University of Surrey ethics committee and all subjects gave written informed consent.

Kinematic data were recorded to quantify the maximum active and passive internal and external rotations of the GHJ for the subject's dominant arm at 60°, 90° and 120° of humerothoracic elevation in the Coronal, Scapular and Sagittal planes. The Scapular plane was defined as 30° anterior to the Coronal plane, measured using a goniometer, and the elevation angle was measured using an inclinometer (SignalQuest Inc., Lebanon). The protocol used to collect kinematic data has been previously presented[15] and the experimental setup is shown in Figure 1. In short: subjects were seated in a restraint chair and the position of their arm was maintained using a tripod and splint. Active axial rotation was measured at a subject-defined, comfortable, consistent speed of internal-external rotation and maximum range was defined by the subject. During passive rotation, a torque was applied in a controlled way and monitored at the distal humerus using a transducer (Applied Measurement Ltd., Aldermaston); the maximum passive range corresponded to a torque of 4Nm in the internal and external directions. Using this setup, variation in maximum internal and external rotation due to experimental factors was minimised[15]; although, as the subject was seated, maximum internal rotation could not be achieved at 60° elevation in the Sagittal plane.

A six degree of freedom marker set was used to acquire kinematic parameters. Reflective markers were positioned at bony landmarks of the humerus and digitised for the scapula, at positions according to recommendations by the International Society of Biomechanics[38]. The motion of the humerus and scapula were recorded by tracking the movement of clusters attached to the segments. The position of the clusters was calibrated at each humeral position, relative to the anatomical landmarks of each segment. An optical motion tracking system (Qualisys, Gothenburg) of 11 cameras recorded the movement of each segment. Segment coordinate systems were defined according to the recommended standard[38] and angles of rotation of the GHJ were computed using Euler sequence YX'Y''[38].

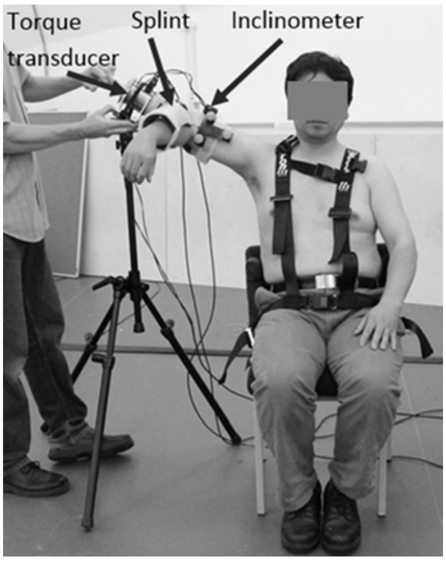

Figure 1: Set-up used during kinematic data collection to measure the maximum angle of active and passive internal and external rotation at multiple humeral positions.

Bone geometrical parameters were acquired from MRI scans of the subject's dominant shoulder at the Royal Surrey County Hospital. Data were recorded using a 3-T scanner (Siemens, Camberley) and a surface array coil was fitted to the shoulder during the scan. The subject lay in the MRI tube in a supine position with their arm at 0º adduction, externally rotated and their elbow extended. The scapula and humerus were scanned in three-dimensions (3D) using a series of two-dimensional (2D) images (slices) acquired in the Coronal plane[10,20,40]. The scapula and proximal humerus were scanned in high resolution (1mm) with slices aligned with the Coronal plane acquired every 1mm[20,40]. The whole humerus was scanned with a high resolution (1mm) in the Coronal plane.

Bone geometrical parameters

The humerus and scapula were segmented in the scans using a greyscale threshold painted region in ScanIP (Version 4, Simpleware, Exeter). Regions were smoothed using a 1mm Recursive Gaussian filter to reduce noise and a 3D model of the humerus and scapula was created[31,40].

Two-dimensional geometrical parameters of the glenoid, articular cartilage and acromion were obtained to describe the shape of the humerus and scapula surrounding the GHJ. Parameters were obtained from 2D slices of the scapula and proximal humerus[10] in ScanIP. Each slice was selected manually, on three different days by two different observers to avoid bias. The slice used to measure geometrical parameters was the average of the manually selected slices. Geometrical parameters of the glenoid were obtained in the plane of the scapula, defined as the plane through the anatomical landmarks of the scapula (Acromial angle (AA), Inferior angle (AI) and root of the scapula spine (TS)). The shape of the glenoid was described using the parameters in Figure 2a and Table 1, obtained from the slice which showed the greatest glenoid height, for consistency. The geometrical parameters of the humeral head shown in Figure 2b and Table 1 were also acquired in the plane of the scapula in the slice which showed the greatest coverage of articular cartilage over the humeral head. Geometrical parameters of the acromion, shown in Figure 2c and Table 1 were obtained in the Sagittal plane, in the slice which showed greatest acromion length. The height, setback and inclination of the coracoid was measured in the transverse plane, in the slice which first showed the complete coracoid process.

Table 1: Geometrical parameters measured in the Scapular (Sc) and Sagittal (S) planes and in three-dimensions (3D) from the subject's bone model of the scapula and proximal humerus. Previous studies which have also used these geometrical parameters are listed. The ID values reference to Figure 2 which illustrates these parameters.

Parameter		Definition	Plane	ID
Glenoid	Depth of glenoid cavity	Distance between humeral head surface and glenoid surface[13]	Sc	i
	Superior depth	Distance between most medial point of the glenoid and most lateral point of the superior glenoid[10]	Sc	ii
	Inferior depth	Distance between most medial point of the glenoid and most lateral point of the inferior glenoid[10]	Sc	iii
	Height	Distance between the most lateral points of the superior and inferior glenoid[6,10,26]	Sc	iv
	Arc of enclosure	Angle subtended by tangents at the most superior and inferior edges of the glenoid, measured at the centre of the humeral head[24]. Best-fit circle used to predict humeral head centre.	Sc	v
	Radius of curvature	Radius of the best fit circle fitted to the surface of the glenoid[24,26]	Sc, 3D	vi
Articular cartilage	Head diameter	Diameter of the humeral head	Sc, 3D	vii
	Diameter	Distance between superior and inferior edges of cartilage[1]	Sc	viii
	Height	Maximum height of the articular cartilage[1]	Sc	ix
	Radius of curvature	Radius of the best fit circle fitted to the articular cartilage[24]	Sc, 3D	x
	Inclination	Angle between humeral shaft axis and axis of the humeral neck[1,12]	Sc, 3D	xi
Acromion	Subacromial depth	Distance between most posterior point of the acromion's anterior surface and the most posterior point on the humeral head[3,37]	S	xii
	Setback	Distance between the most inferior points of the acromion and the humeral head.	S	xiii
	Length	Distance between the most superior and inferior acromion edges[37]	S	xiv

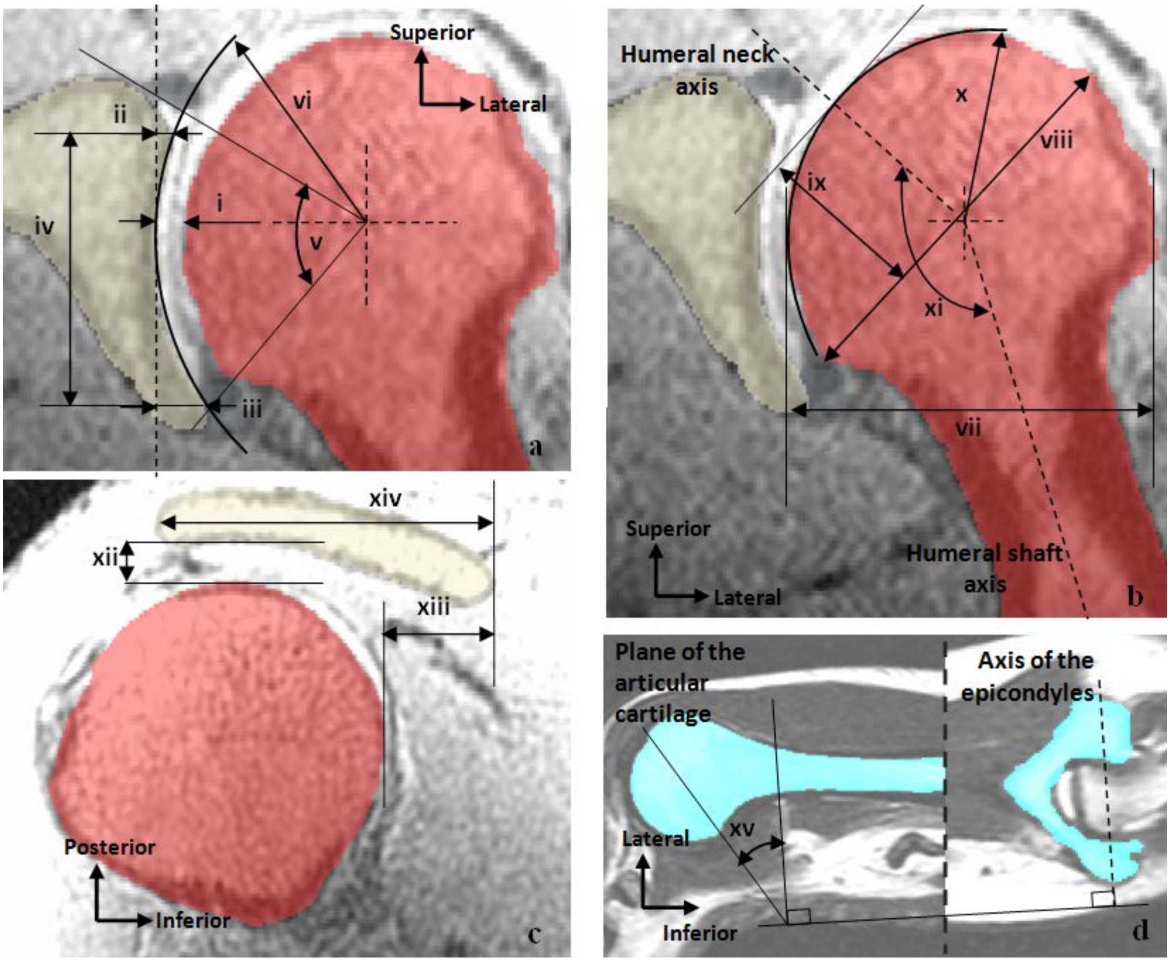

Figure 2: Geometrical parameters of the glenoid (a), humeral head (b), acromion (c) and an illustration of the definition of humeral retroversion (d). Geometrical parameters are listed in Table 1.

Some geometrical parameters (shown in Table 1) were also measured in three-dimensions from the bone models of each subject using 3-matic Research software (9.0, Materialise, Leuven). In the bone model of the scapula and proximal humerus, the radii of curvature were measured by fitting a best-fit sphere to the surface of the model; whilst the humeral inclination was measured using a linear best-fit tool to approximate the humeral shaft axis and the humeral neck axis. The angle of humeral retroversion (xv) shown in Figure 2d was measured from the 3D model of the humerus, defined as the angle subtended between the axis of the epicondyles and the plane of the articular surface[21,28]. The axis of the epicondyles was defined by fitting a best-fit cylinder to the epicondyle surface.

Geometrical parameters were normalised with respect to the size of the bones to allow parameters to be compared between individuals without the effect of size[18,39]. The geometrical parameters of the glenoid and scapula were normalised to the height of the scapula and geometrical parameters of the humerus were normalised to the length of the humerus. A matrix of Pearson product moment correlation coefficients (significance level of 0.05) was used to investigate correlation between the measures of bone geometry and the maximum active and passive internal and external rotations of the GHJ.

Weighted least squares regression expressions were used to predict the maximum active and passive internal and external rotation of the GHJ from the geometric parameters of the bones[40]. The weighted linear regression expressions were derived at each humeral position, each consisting of up to three geometrical parameters. The parameters and their weightings used in the expressions were defined such that the predicted range of axial rotation was most comparable to the quantified axial rotational range. A leave-one-out experiment[39] was used to establish whether the weighted expressions of geometrical parameters could be used to predict the range-of-motion of the GHJ[39]. A four-factor repeated analysis of variance (ANOVA) was used to find differences between the predicted and quantified range (internal and external) at each humeral elevation angle and elevation plane during active and passive motion. When differences were significant ($p<0.05$), a Posthoc test with Bonferroni correction was used to establish the influence of each of these independent factors.

Collision detection simulation

The subject-specific bone models of the scapula and humerus were imported into SolidEdge software (Version 7, Siemens, Camberley) to simulate rotations of the bones and identify any regions of bony collision at positions of maximum internal and external rotation. These observations were used to confirm the previously calculated correlations between axial range-of-motion and bone geometrical parameters and observe the region(s) of collision which affect the range-of-motion of the GHJ. To identify points of bony collision during internal and external rotation at each humeral position, the model of the humerus was rotated relative to the scapula to simulate the 60°, 90° and 120° humerothoracic elevation angles in the Coronal, Scapular and Sagittal planes. The model of the humerus was rotated relative to the scapula using the glenohumeral plane and elevation angles recorded during the subject's kinematic data collection session as the MRI scans were acquired at a single humeral position and did not include the thorax. Anatomical coordinate systems of the humerus and scapula were defined in the bone model to enable the humerus to be rotated relative to the scapula. Three anatomical landmarks of each bone were used to define the bone's coordinate system. The plane of the scapula (landmarks AA, AI and TS) was assumed to represent the Scapular plane; and the plane of the humerus (epicondyles and centre of the humeral head) was assumed to represent the Coronal plane of the humerus.

During active rotations, the centre of rotation of the humeral head was fixed on the glenoid surface, simulating muscle forces and joint compression[17]. During passive rotations, the humeral head could translate by up to 3mm in the superior, inferior and lateral directions, simulating translations that occur when the GHJ is not compressed [11,17].

The humerus was rotated to the angle of maximum internal and external rotation in the subject-specific bone model using the glenohumeral angle of maximum internal and external rotation quantified from the subject's kinematic data. Points of bony collision were highlighted in the model using automatic interference detection during rotation, showing which bony restraints affected the maximum internal and external rotation of the GHJ at each humeral position.

Results

The axial rotational range of the GHJ quantified from the kinematic data of the 10 healthy subjects are shown in Supplementary table 1 and Supplementary table 2 shows the average bone geometrical parameters measured from the subject's MRI scans.

Correlation between geometrical parameters and range-of-motion

Bone geometrical parameters were correlated with the maximum internal and external rotation of the GHJ. Tables 2 and 3 list the geometrical parameters which show strongest correlation with the maximum internal and external rotation at each humeral position. The matrix of correlation coefficients for each geometrical parameter is shown in the Supplementary tables 3 and 4. The maximum internal rotation at 60° elevation in the Sagittal plane was not achieved as this was limited while the participant was seated during kinematic data collection.

The geometrical parameters affecting the axial rotational range were dependent on the plane of elevation and the elevation angle of the humerus. In the Scapular plane, maximum internal rotation showed greatest correlation with the glenoid curvature and the glenoid depth. Glenoid curvature showed greatest correlation at 60° elevation ($r=0.76$, $p<0.01$). A greater height of articular cartilage correlated with greater external rotation at 60° elevation in the Scapular plane ($r=0.63$, $p<0.05$), but it showed less significant or no correlation at higher humeral elevations. A greater superior depth of the glenoid was correlated with a greater internal rotation at 120º elevation ($r=0.82$, $p<0.01$) in the Scapular plane.

In the Sagittal plane, external rotations at low elevations were greater when the coracoid surface was orientated away from the humeral head. A greater maximum passive internal rotation was achieved with a greater glenoid height and a greater arc of enclosure. The radius of curvature of the articular cartilage limited maximum internal and external rotation in the Sagittal plane, with greatest correlation at 90º elevation ($r=0.75$, $p<0.01$). The glenoid arc of enclosure showed strongest correlation at 120° elevation ($r=0.72$, $p<0.01$).

Internal-external rotations at 120° humeral elevation correlated with the shape of the acromion and glenoid. Active external rotation was limited by the length and setback of the acromion, where the greatest correlation was observed in the Coronal plane ($r=-0.64$, $p<0.05$). The results showed that a shorter acromion, positioned more superiorly correlated with a greater external rotation. The superior depth of the glenoid showed strongest correlation ($r=0.72$, $p<0.01$) during passive internal rotation at 120° humeral elevation in the Scapular and Sagittal planes.

When comparing the geometrical parameters measured in 3D, the results showed no significant difference to measurements obtained in two-dimensions. Therefore, when investigating correlation with axial rotational range, only the 2D measurements are presented in the tables.

Table 2: Geometrical parameters which showed greatest correlation with the active internal and external rotation at each humeral position. (* $p<0.05$; ** $p<0.01$). At 60° elevation in the Sagittal plane, maximum internal rotation was not achieved.

Humeral elevation angle (°) and plane		Internal		External	
		Bone geometry parameter	**r**	**Bone geometry parameter**	**r**
Coronal	**60**	Acromion length	0.64*	Humeral head diameter Glenoid arc of enclosure	0.74** 0.69**
Coronal	**90**	Subacromial depth Glenoid curvature	0.74** 0.69**	Articular cartilage curvature	0.54*
Coronal	**120**	Humeral inclination	-0.63*	Acromion setback Glenoid curvature	-0.64* 0.62*
Scapular	**60**	Glenoid curvature Inferior glenoid depth	0.76** 0.76**	Articular cartilage height	0.63*
Scapular	**90**	Glenoid curvature	0.58*	Subacromial depth Glenoid height	0.67** 0.65*
Scapular	**120**	Superior glenoid depth Glenoid curvature	0.82** 0.64*	Acromion length	-0.63*
Sagittal	**60**			Coracoid inclination	-0.69**
Sagittal	**90**	Articular cartilage curvature	0.75**	Articular cartilage curvature Articular cartilage height	0.67** 0.61*
Sagittal	**120**	Glenoid arc of enclosure Articular cartilage curvature	0.72** 0.71**	Glenoid height Acromion setback	-0.61* -0.61*

Table 3: Geometrical parameters which showed greatest correlation with the passive internal and external rotation at each humeral position. (* $p<0.05$; ** $p<0.01$). At 60° elevation in the Sagittal plane, maximum internal rotation was not achieved.

Humeral elevation angle (°) and plane		Internal		External	
		Bone geometry parameter	**r**	**Bone geometry parameter**	**r**
Coronal	**60**	Glenoid depth	0.58*	Glenoid depth	-0.53*
Coronal	**90**	Subacromial depth Humeral retroversion	0.71** -0.66**	Inferior glenoid depth Acromion setback	-0.60* -0.59*
Coronal	**120**	Humeral retroversion Glenoid arc of enclosure	-0.61* 0.59*	Acromion length	-0.58*
Scapular	**60**	Inferior glenoid depth Humeral retroversion	0.87** -0.72**	Acromion setback Articular cartilage height	-0.60* 0.55*
Scapular	**90**	Subacromial depth Superior glenoid depth	0.65* 0.64*	Glenoid arc of enclosure Subacromial depth	0.72** 0.66*
Scapular	**120**	Superior glenoid depth Glenoid arc of enclosure	0.72** 0.67*	Acromion length	-0.68*
Sagittal	**60**			Coracoid inclination	-0.42*
Sagittal	**90**	Subacromial depth Superior glenoid depth	0.74** 0.64*	Acromion setback Coracoid inclination	-0.52* -0.67**
Sagittal	**120**	Glenoid arc of enclosure	0.72**	Glenoid height	-0.60*

				Superior glenoid depth	0.72**	Acromion setback	-0.57*

Weighted linear regression expressions were derived from geometrical parameters to predict the maximum axial range-of-motion at each humeral position. The expressions which show the closest approximation to the quantified axial rotational range are shown in Table 4 for active and passive motion in the form given in Equation 1. Each weighted expression included up to three geometric parameters (Var1-Var3) and their weighted constants (C1-C4). The general equation is:

$$(C1 \times Var1) + (C2 \times Var2) + (C3 \times Var3) + C4 \qquad \text{Equation 1}$$

And the geometric parameters and constants for various expressions are given in Table 4.

Using the leave-one-out experiment[39], the results showed there was no significant difference (p=0.15) between the range-of-motion quantified from an individual's kinematic data and the range-of-motion predicted using the weighted linear regression expressions.

Table 4: Weighted linear regression expressions derived at each humeral position to predict the maximum active and passive axial range-of-motion.

Humeral position (Plane, elevation)		Active C1	Active Var1	Active C2	Active Var2	Active C3	Active Var3	Active C4	Passive C1	Passive Var1	Passive C2	Passive Var2	Passive C3	Passive Var3	Passive C4
Coronal	**60**	9.6	Cartilage height	0.2	Humeral retroversion	-1.4	Cartilage curvature	38.6	-7.3	Glenoid depth	-0.4	Glenoid depth inferior	-.7	Humeral retroversion	213.5
	90	3.2		0.5		0.4		89.2	-5.9		-4.6		0.4		244.1
	120	-2.9		0.4		2.8		108.1	1.5		-1.8		0.9		156.2
Scapular	**60**	-0.6	Acromion length	-2.3	Subacromial depth	0.0	Glenoid curvature	191.4	-0.8	Glenoid depth inferior	-1.3	Acromion length	-4.6	Subacromial depth	312.5
	90	-1.0		-1.3		0.1		207.1	-0.1		-1.0		-4.5		280.1
	120	-2.8		0.1		-1.9		327.2	-1.8		-2.2		-0.4		287.9
Sagittal	**60**	-2.1	Subacromial depth	-3.8	Cartilage curvature	-1.1	Glenoid arc of enclosure	372.8	-0.3	Subacromial depth	-5.3	Glenoid height	0.4	Cartilage curvature	292.9
	90	-2.1		-4.5		-0.7		361.1	-2.8		-3.4		-2.5		358.4
	120	-4.1		-5.9		-0.5		376.5	-1.7		-2.9		-2.9		331.8

<u>Collision detection</u>

The observations of points of collision in the subject-specific bone models were consistent across all subjects, showing which bony collisions limited the maximum internal and external rotations at each humeral position. During active axial rotations, the shape of the glenoid and articular cartilage were shown to limit the maximum internal and external rotations. In particular, a greater area of coverage of articular cartilage allowed a greater axial rotation to be achieved, as this provided a greater surface to be in contact with the glenoid (Figure 3a). This was observed at maximum internal and external rotation in the Coronal and Sagittal planes. The maximum internal rotation in the Sagittal plane was also limited by collision between the greater tuberosity and the anterior edge of the glenoid. At 60° elevation in the Scapular plane, the maximum internal rotation was limited by collision between the lesser tuberosity and inferior edge of the glenoid and the maximum external rotation limited by the articular cartilage contact area.

Observations during passive axial rotation in each subject's bone model showed that collision initially occurred between the humeral head and the glenoid, but following this the humeral head translated anteriorly/ posteriorly on the glenoid during internal/ external rotations respectively. The translation of the humeral head allowed further internal-external rotation to be achieved before collision with the acromion. The maximum passive internal/ external rotation was therefore limited by a combination of collisions with the glenoid and acromion, as shown in Figure 3b. The movie available as supplementary material provides further details of the points of bony collision during passive motion across the range of motion of the GHJ.

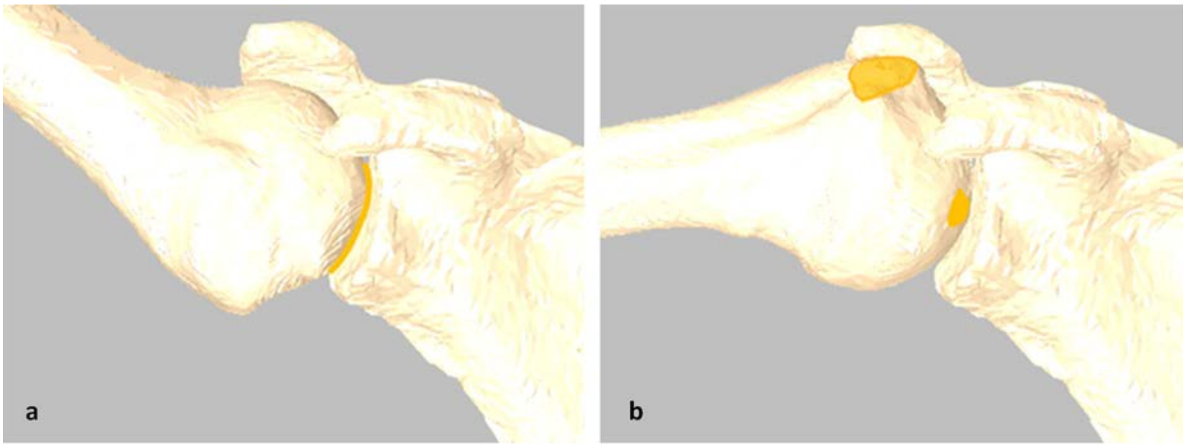

Figure 3: Observations from collision detection, showing the region of contact (highlighted line) between the articular cartilage and glenoid, which limited the maximum active internal rotation at 120º in the Coronal plane (a). Maximum passive external rotation at 90° elevation in the Scapular plane is limited by a combination of collision between the humeral head and the posterior edge of the glenoid and between lesser tuberosity and posterior-lateral edge of the acromion, shown by the highlighted points (b).

Discussion

Bony constraints between the humerus and scapula are shown to limit the maximum internal and external rotation of the GHJ. Points of bony collision depend on the position of the humerus and contribute towards variation in the range of axial rotation between individuals. Correlations between bone geometrical parameters and the axial rotational range-of-motion and the observed points of collision showed that active axial rotations were limited by the shape of the acromion, articular cartilage and glenoid, and during passive rotations, the range of motion was limited by the shape of the glenoid and acromion. Understanding the bony constraints of the GHJ can be used to improve the positioning of shoulder implants during pre-operative planning, allowing a more natural range-of-motion to be achieved. It also allows the normal range-of-motion of the joint to be predicted for an individual, allowing more realistic patient specific rehabilitation targets to be set.

The quantified ranges of motion of the GHJ were supported by the results of previous data collected using the same kinematic protocol[15] at each humeral position. The geometrical parameters were also comparable to those reported in previous studies, including the geometrical parameters of the humeral head[10,12,16], glenoid[10,13,24] and acromion[3,37]. However, some parameters, such as the radius of the humeral head may have been underestimated in previous studies (24mm[12] and 22mm[10]) compared to 30mm which was measured in the present study. This is likely due to the choice of the slice used to measure the humeral head diameter, as these previous studies have acquired the radius from a slice which showed the greatest glenoid height, rather than the greatest humeral head diameter. The parameters presented in this study were measured in a consistent slice and anatomical plane, and normalised to the size of the bones for all participants; hence, variation in the quantified parameters was a result of variation in shape between individuals and not due to differences in size. Correlation between the geometrical parameters and range of axial rotation of the

GHJ enabled the bony constraints of the GHJ to be investigated. The significant correlations between the axial rotational range and geometrical parameters were supported by observations of points of collision from the subject-specific bone model simulations at multiple humeral positions.

A greater active range-of-motion was correlated with a greater height and curvature of the articular cartilage and glenoid, and a greater subacromial depth. The shape of the acromion, articular cartilage and glenoid are therefore important to consider when improving or predicting the normal range of axial rotation of the GHJ at low elevations in the Coronal, Scapular and Sagittal planes. However, in the Sagittal plane, collision between the greater tuberosity and the anterior edge of the glenoid is more likely, thus leading to a reduced range of axial rotation in the Sagittal plane compared to the Coronal and Scapular planes.

The passive range of motion was greater than the corresponding active range of motion at each humeral position due to the translation of the humeral head on the glenoid. Previous studies have found that the shape of the glenoid surface, in particular the radius of curvature and glenoid depth affects the translation of the humeral head[17], hence these parameters also affect the range of passive axial rotation of the GHJ. Maximum passive internal-external rotations were shown to be limited by the shape of the glenoid and acromion, where a greater glenoid and subacromial depth and a shorter and more superiorly positioned acromion were correlated with a greater passive axial rotational range. Bony collision between the humeral head and acromion was also shown to limit the maximum angle of humeral abduction in an in-vitro study by Krekel *et al.*[20]. Lewis *et al.* also suggested that the shape of the acromion affects the range-of-motion of the GHJ, where a laterally orientated acromion may lead to a reduced range-of-motion at higher elevations[23].

At higher humeral elevations, external rotation was frequently limited by collision between the lesser tuberosity and the posterior-lateral edge of the acromion, meaning a shorter acromion, positioned more superiorly would enable a greater external rotation to be achieved. This is in agreement with the results reported by Chopp-Hurley *et al*., whose probabilistic model of variation in the subacromial depth showed that soft-tissue impingement between the humeral head and acromion may limit the range-of-motion at higher humeral elevations[5]. Variation in the position of the acromion relative to the humeral head leads to differences in the maximum external rotation between individuals and is also an important restraint in limiting the range of axial rotation at higher humeral elevations. The bony collisions with the acromion means the range of axial rotation is reduced at 120° humeral elevations, which was also suggested by Lewis *et al*. when they investigated differences in the shape of the humerus and scapula in apes and humans[23]. It is therefore important to consider the shape of the acromion when characterising an individual's range of axial rotation at higher humeral elevations.

Previous studies investigating the range-of-motion of the GHJ in overhead sports groups found osseous adaptations leading to an increased angle of retroversion following repeated high stresses at the joint during regular overhead sports activities[4,7,30,34]. Conversely, in the normal population, when there are no osseous adaptations, the results showed the acromion shape is more likely to limit the maximum external rotation that can be achieved at high humeral elevations.

This improved understanding of the bony restraints of the GHJ can be used in future studies concerned with improving the positioning and design of shoulder implants, to allow a greater and more natural range of motion to be achieved. One example of such use is demonstrated in the study by Krekel *et al*., where a subject-specific segmented bone model of the shoulder was used to predict the range of motion of the joint in pre-surgical planning[20]. In these simulations, the authors showed that a change in the position of the humeral head can allow a greater range of motion to be achieved[19,20]. The present study provides further understanding of the points of collision at multiple humeral positions and the findings presented here are strengthened by the presentation of *in-vivo* kinematics assessments of the achieved ranges of motion using the same subject group. Thus, the present study does not make assumptions regarding the achieved ranges of motion based on bone model simulations but rather seeks to understand the relationship between bone osteology and joint range of motion.

The range of the internal and external rotation of the shoulder is of clinical and functional importance. In the clinic, the axial rotational range is used in shoulder examinations to test for pain and instability of the shoulder[25] and the external rotation is often used as a clinical outcome measure[2,8]. Previous studies have also documented losses in the range of internal and external rotation in patients with various shoulder pathologies[2,32,36]. This loss is associated with a significant loss of function[8,33], because of the role the axial rotational range plays in performing activities of daily living, such as hair combing and washing the back[35]. Despite the frequent use of this range of motion in clinical examination[25] and functional assessment[2], the internal and external ranges of motion are variable between individuals[15]. In this study, measurements of bone geometry were used to define weighted linear regression expressions that can now be used to predict an individual's axial rotational range in the absence of pathology. The predicted range of motion was shown to be comparable to the quantified range of motion at each humeral position when using the weighted linear regression expressions. However, expressions combining geometrical parameters which provided a less optimal prediction are not presented in the study. Alternatively, a stepwise regression analysis using backward elimination or a non-linear approach could have been used to identify the geometrical parameters to use in the expressions.

It is important to note that the range-of-motion of the GHJ may be limited by a combination of multiple bony constraints, soft-tissue impingement and ligament wrap lengths, which may explain why the range-of-motion had moderate or no correlation with geometrical parameters at some humeral positions. The study measured the geometrical parameters of the bone, but the low contrast between regions of the MRI scans would not facilitate the segmentation of the muscles and ligaments of the GHJ[29]. Therefore, soft-tissue impingement could not be investigated using the current model. An in-vitro study by Karduna *et al*. investigated the role of the soft-tissue restraints during active and passive positioning of the humerus at maximum internal and external rotation[17]. Their study showed that muscle forces were likely to limit humeral head translations and the range-of-motion of the joint. The Glenohumeral ligament wrap length has also been shown to limit the maximum passive internal-external rotation of the GHJ[17,27].

Although there were a relatively small number of participants in the study, the quantified angles of axial rotation and geometrical parameters were comparable to those reported in previous studies. No participants had previous shoulder injury and did not regularly participate in overhead sports; hence bone geometry of the GHJ is unlikely to have undergone significant osseous adaptations. The participants were also from a younger age group, so the results may not be generalisable to older populations or other sports populations.

In the kinematic data collection, the effects of skin artefact were minimised by using clusters and calibrating at each humeral position, as described previously[15]. When creating the bone models for each participant, the segmented regions were smoothed to reduce noise and improve the quality of the bone surface without causing excessive shape modifications, ensuring geometrical parameters provided an accurate measurement of bone geometry.

Geometrical parameters were acquired in the anatomical planes of the bones to account for differences in the position of the subject during the scan. However, the shoulder was imaged at a single humeral position; hence the measurements could not be used to investigate how some geometrical parameters, such as the glenoid depth or subacromial depth changed with humeral position. However, the bone model enabled these constraints to be simulated during internal-external rotation at each humeral position, based on the quantified angles of rotation from the kinematic measurements.

In conclusion, the maximum internal and external rotations of the GHJ are shown to be limited by bony constraints. The constraints were dependent on the elevation angle and elevation plane of the humerus. Bone geometrical parameters of the humerus and scapula which showed statistically significant correlation with the maximum internal and external rotation corresponded to observations of collision in the subject-specific bone models. In general, active rotations were limited by the curvature of the glenoid and articular cartilage and the area of contact between the humeral head and glenoid; whilst passive rotations were limited by the shape of the acromion. This meant that at high humeral elevation angles a shorter acromion and greater subacromial depth allowed a greater range of axial rotation to be achieved.

References

1. Boileau P, Walch G. The three-dimensional geometry of the proximal humerus. *J Bone Joint Surg*. 1997; 79B(5): 857-865. PMID: 9331050
2. Bryant D, Litchfield R, Sandow M, Gartsman GM, Guyatt G, Kirkley A. A comparison of pain, strength, range of motion, and functional outcomes after hemiarthroplasty and total shoulder arthroplasty in patients with osteoarthritis of the shoulder. *J Bone Joint Surg Am.* 2005; 87(9): 1947-1956. PMID: 16140808

3. Cay N, Tosun Ö, Doğan M, Karaoğlanoğlu M, Bozkurt M. The effect of morphometric relationship between the glenoid fossa and the humeral head on rotator cuff pathology. *Acta Orthop Traumato*. 2012; 46(5): 325-331. PMID: 23268816
4. Chant CB, Litchfield R, Griffin S, Thain LMF. Humeral Head Retroversion in Competitive Baseball Players and Its Relationship to Glenohumeral Rotation Range of Motion. *J Orthop Sport Phys*. 2007; 37(9): 514-520. PMID: 17939610
5. Chopp-Hurley JN, Langenderfer JE, Dickerson CR. A probabilistic orthopaedic population model to predict fatigue-related subacromial geometric variability. *J Biomech*. 2016; 49(4): 543-549. PMID: 26857990
6. Churchill RS, Brems JJ, Kotschi H. Glenoid size, inclination, and version: An anatomic study. *J Shoulder Elbow Surg*. 2001; 10(4): 327-332. PMID: 11517362
7. Crockett HC, Gross LB, Wilk KE, et al. Osseous adaptation and range of motion at the glenohumeral joint in professional baseball pitchers. *Am J Sports Med*. 2002; 30(1): 20-26. PMID: 11798991
8. Eriks-HooglandIE, de Groot S, Post MW, van der Woude LH. Correlation of shoulder range of motion limitations at discharge with limitations in activities and participation one year later in persons with spinal cord injury. *J Rehabil Med*. 2011; 43(3): 210-215. PMID: 21305236
9. Gibbons LJ. Managing acute shoulder injuries in the emergency department. *Emerg Nurse*. 2014; 22(6): 20-29. PMID: 25270818
10. Gielo-Perczak K, Matz S, An K-N. Arm abduction strength and its relationship to shoulder geometry. *J Electromyogr Kines*. 2006; 16: 66-78. PMID: 16129621
11. Harryman II DT, Sidles JA, Clark JM, McQuade KJ, Gibb TD, Matsen III FA. Translation of the humeral head on the glenoid with passive glenohumeral motion. *J Bone Joint Surg Am*. 1990; 72(9): 1334-1343. PMID: 2229109

12. Hertel R, Knothe U, Ballmer FT. Geometry of the proximal humerus and implications for prosthetic design. *J Shoulder Elbow Surg*. 2002; 11: 331-338. PMID: 12195250

13. Howell SM, Galinat BJ. The glenoid-labral socket. A constrained articular surface. *Clin Orthop Relat R*. 1989; 243: 122-125. PMID: 2721051

14. Hughes PC, Green RA, Taylor NF. Measurement of Subacromial Impingement of the Rotator Cuff. *J Sci Med Sport*. 2012; 15(1): 2-7. PMID: 21856224

15. Humphries A, Cirovic S, Bull A, Hearnden A, Shaheen A. Assessment of the Glenohumeral joint's active and passive axial rotational range. *J Shoulder Elb Surg*. 2015; 24: 1974-1981. PMID: 26410346

16. Iannotti JP, Gabriel JP, Schneck SL, Evans BG, Misra S. The normal glenohumeral relationships. An anatomical study of one hundred and forty shoulders. *J Bone Joint Surg Am*. 1992; 74: 491-500. PMID: 1583043

17. Karduna AR, Williams GR, Williams JL, Iannotti JP. Kinematics of the glenohumeral joint: influences of muscle forces, ligamentous constraints, and articular geometry. *J Orthopaed Res*. 1996; 14: 986-993. PMID: 8982143

18. Kendall DG. The diffusion of shape. *Adv App Probab*. 1977; 9(3): 428-430.

19. Krekel PR, Botha CP, Valstar ER, de Bruin PW, Rozing PM, Post FH. Interactive simulation and comparative visualisation of the bone-determined range of motion of the human shoulder. *Proceedings of Simulation and Visualization*. 2006; 275-288.

20. Krekel PR, de Bruin PW, Valstar ER, Post FH, Rozing PM, Botha CP. Evaluation of bone impingement prediction in preoperative planning for shoulder arthroplasty. *Proc Inst Mech Eng H*. 2009; 223(7): 813-822. PMID: 19908420

21. Kronberg M, Broström LA, Söderlund V. Retroversion of the humeral head in the normal shoulder and its relationship to the normal range of motion. *Clin Orthop Relat Res*. 1990; 253: 113-117. PMID: 2317964

22. Labriola JE, Lee TQ, Debski RE, Mcmahon PJ. Stability and Instability of the Glenohumeral Joint: The Role of Shoulder Muscles. *J Shoulder Elbow Surg*. 2005; 14(1): S32-S38. PMID: 15726085
23. Lewis J, Green A, Yizhat Z, Pennington D. Subacromial Impingement syndrome: Has evolution failed us? *Physiotherapy*. 2001; 87: 191-198.
24. McPherson EJ, Friedman RJ, An YH, Chokesi R, Dooley RL. Anthropometric study of normal glenohumeral relationships. *J Shoulder Elbow Surg*. 1997; 6(2): 105-112. PMID: 9144597
25. Moen MH, de Vos RJ, Ellenbecker TS, Weir A. Clinical tests in shoulder examination: How to perform them. *Br J Sports Med*. 2010; 44(5): 370-375. PMID: 20371563.
26. Moineau G, Levigne C, Boileau P, Young A, Walch G, The French Society for Shoulder & Elbow (SOFEC). Three-dimensional measurement method of arthritic glenoid cavity morphology: Feasibility and reproducibility. *Orthop Traumatol Surg Res*. 2012; 98(6): S139-145. PMID: 22964089
27. O'Brien SJ, Neves MC, Arnoczky SP, et al. The anatomy and histology of the inferior glenohumeral ligament complex of the shoulder. *Am J Sports Med*. 1990; l8(5): 449-456. PMID: 2252083
28. Pearl ML, Volk AG. Retroversion of the proximal humerus in relationship to prosthetic replacement arthroplasty. *J Shoulder Elbow Surg*. 1995; 4: 286-289. PMID: 8542372
29. Pérez G, Garamendi JF, Montes Diez R, Schiavi E. A multiphase approach to MRI shoulder images classification. In: Fred A, Filipe J, Gamboa H, eds. *Communications in Computer and Information Science*. Berlin: Spinger; 2009: 321-329

30. Reagan K, Meister K, Horodyski MB, Werner DW, Carruthers C, Wilk K. Humeral Retroversion and Its Relationship to Glenohumeral Rotation in the Shoulder of College Baseball Players. *Am J Sport Med*. 2002; 30(3): 354-360. PMID: 12016075
31. Rhoad RC, Klimkiewicz JJ, Williams GR, Kesmodel SB, Udupa JK, Kneeland JB, Iannotti JP. A new in vivo technique for three-dimensional shoulder kinematic analysis. *Skeletal Radiol*. 1998; 27(2): 92-97. PMID: 9526775
32. Rundquist PJ, Ludewig PM. Patterns of motion loss in subjects with idiopathic loss of shoulder range of motion. *Clin Biomech.* 2004; 19(8): 810-818. PMID: 15342153
33. Rundquist PJ, Ludewig PM. Correlation of 3-dimensional shoulder kinematics to function in subjects with idiopathic loss of shoulder range of motion. *Phys Ther*. 2005; 85(7): 636-647. PMID: 15982170
34. Schwab LM, Blanch P. Humeral torsion and passive shoulder range in elite volleyball players. *Phys Ther Sport*. 2009; 10: 51-56. PMID: 19376472
35. Triffitt PD. The relationship between motion of the shoulder and the stated ability to perform activities of daily living. *J Bone Joint Surg Am*. 1998; 80(1): 41-46. PMID: 9469307
36. Tyler TF, Nicholas SJ, Roy T, Gleim GW. Quantification of posterior capsule tightness and motion loss in patients with shoulder impingement. *Am J Sports Med*. 2000; 28(5): 668-673. PMID: 11032222
37. Von Schroeder HP, Kuiper SD, Botte MJ. Osseous anatomy of the scapula. *Clin Orthop Relat R*. 2001; 383: 131-139. PMID: 11210947
38. Wu G, van der Helm FC, Veeger HE, et al. ISB recommendation on definitions of joint coordinate systems of various joints for the reporting of human joint motion–Part II: shoulder, elbow, wrist and hand. *J Biomech*. 2005; 38(5): 981-992. PMID: 15844264

39. Yang Y, Bull AMJ, Rueckert D, Hill A. 3D statistical shape modelling of long bones. In: Pluim JPW, Likar B, Gerritsen FA, eds. *Biomedical Image Registration, WBIR*. Berlin: Spinger; 2006: 306-314.

40. Yang YM, Rueckert D, Bull AMJ. Predicting the shapes of bones at a joint: application to the shoulder. *Comput methods Biomech Biomed Eng*. 2008; 11(1): 19-30. PMID: 17943483

Supplementary video caption:

A video to show the points of bony collision at maximum internal and external passive rotation across the full range-of-motion of the GHJ.